Correspondence to:
M. H. Denton,
m.denton@lancaster.ac.uk

First optical observations of energetic electron precipitation at 4278 Å caused by a powerful VLF transmitter

M. H. Denton[1,2], M. J. Kosch[1,3,4], J. E. Borovsky[1,2], M. A. Clilverd[5], R. H. W. Friedel[6], and T. Ulich[7]

[1]Department of Physics, Lancaster University, Lancaster, UK, [2]Space Science Institute, Boulder, Colorado, USA, [3]South African National Space Agency, Hermanus, South Africa, [4]University of KwaZulu-Natal, Durban, South Africa, [5]British Antarctic Survey, Cambridge, UK, [6]ISR-1, Los Alamos National Laboratory, Los Alamos, New Mexico, USA, [7]Sodankylä Geophysical Observatory, Sodankylä, Finland

Abstract A summary is presented of experimental optical observations at 4278 Å from close to a powerful (~150 kW) VLF transmitter (call sign JXN) with a transmission frequency of 16.4 kHz. Approximately 2.5 s after transmitter turn-on, a sudden increase in optical emissions at 4278 Å was detected using a dedicated camera/charge-coupled device (CCD) monitoring system recording at a frequency of 10 Hz. The optical signal is interpreted as a burst of electron precipitation lasting ~0.5 s, due to gyro-resonant wave-particle interactions between the transmitted wave and the magnetospheric electron population. The precipitation was centered on the zenith and had no detectable spatial structure. The timing of this sequence of events is in line with theoretical predictions and previous indirect observations of precipitation. This first direct measurement of VLF-induced precipitation at 4278 Å reveals the spatial and temporal extent of the resulting optical signal close to the transmitter.

1. Introduction

The Earth's outer radiation belt consists of trapped high-energy electrons whose motion results from a combination of their bounce, gyration, and drift, along, around, and perpendicular to, the magnetic field, **B**, respectively. The discovery of the radiation belts [*Van Allen et al.*, 1958] and subsequent descriptions of the large-scale physical processes operating in the region [e.g., *Hess*, 1968, and references therein] have been followed by attempts to understand, model, and predict the natural variation of electrons which make up the outer belt. Various acceleration and loss mechanisms have been suggested to explain the variation in the measured electron flux in the outer belt, which can change by orders of magnitude over time scales as short as a few minutes [*Baker et al.*, 1994]. Interest in the radiation belts remains high owing to the damaging effect these electrons can have upon spacecraft [e.g., *Wrenn*, 2009]. Most communications satellites spend at least part of their time within the radiation belts requiring satellite designers to include costly shielding on sensitive instrumentation to mitigate the effect of incident electrons and ions.

One natural loss mechanisms for radiation belt electrons is related to the occurrence of whistler-mode chorus waves [*Dungey*, 1963; *Helliwell et al.*, 1973]. Via cyclotron resonance, whistler-mode chorus waves cause pitch angle scattering of electrons. This results in the temporal decay of the number of electrons—scattered electrons penetrate deeper into the atmosphere where losses are more likely. Hence, over time, the number of electrons will decrease as a result. The first suggestion that electrons could be lost from the radiation belts via cyclotron-resonant interactions was (remarkably) accompanied by a prediction that the same population could be artificially removed with radio wave transmitters; *If…the failure of whistlers to remove the trapped radiation…is due to lack of power…it may be asked whether man-made transmitters can do better* [*Dungey*, 1963]. Numerous studies have since suggested mechanisms to carry out this process—namely the artificial reduction of damaging fluxes of energetic electrons [e.g., *Bell et al.*, 1985; *Inan et al.*, 1985; *Abel and Thorne*, 1998; *Rodger et al.*, 2006].

The most powerful ground-based radio transmitters, with transmission frequencies of the order predicted for radiation belt electron cyclotron resonance, are VLF transmitters used for land-to-submarine communications [*Koons et al.*, 1981]. Electron precipitation into the atmosphere near such transmitters has indeed been modeled [e.g., *Inan et al.*, 1984; *Marshall et al.*, 2010] with supporting evidence for such
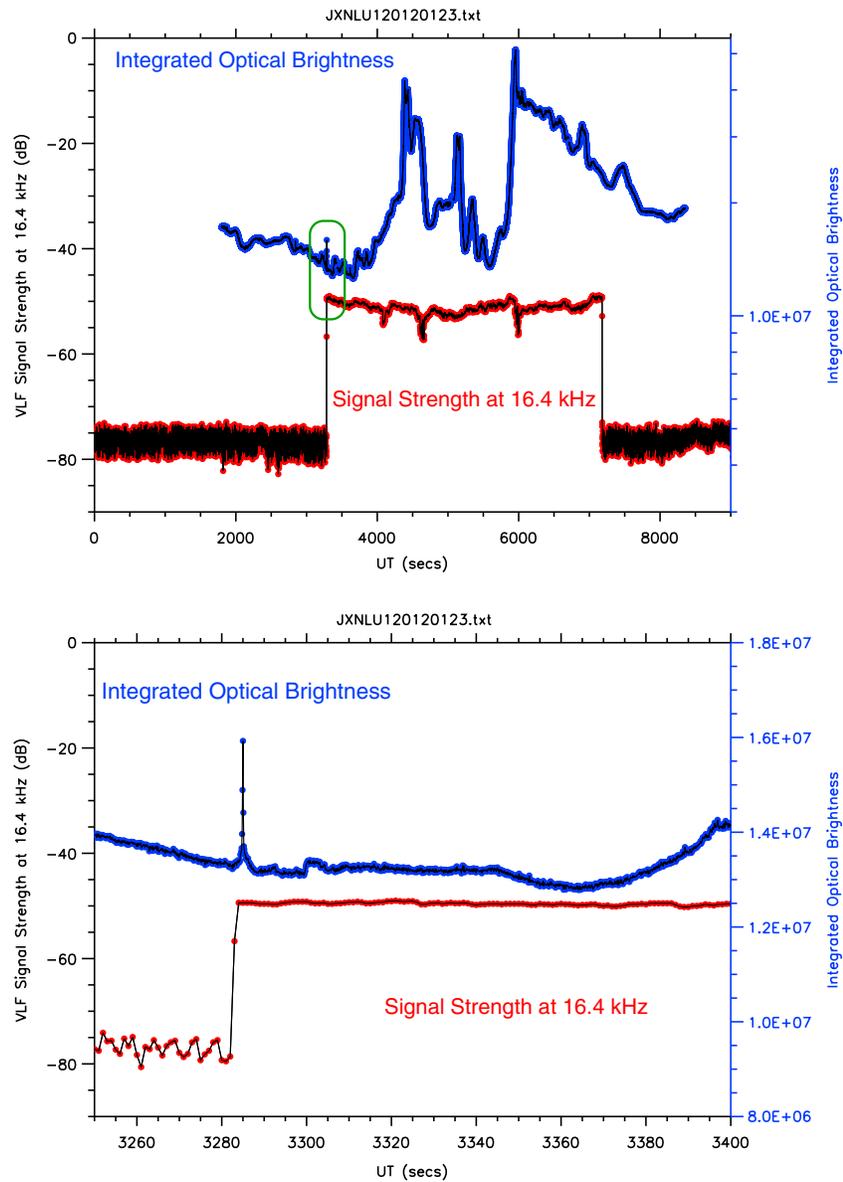
Figure 1. Showing the measured VLF signal strength at 16.4 kHz (left axis - red dots) and the measured integrated optical brightness at 4278 Å (right axis - blue dots) as a function of time in seconds, for observations on the 23 January 2012. The field-of-view is approximately ±15° which corresponds to ~26 km in the sky at 100 km altitude. (top) All data on recorded during this period with the green box highlighting the time around transmitter turn-on. (bottom) An enlarged view of 150 s around the time of transmitter turn-on with the standard error of the mean shown by the blue-dashed line.

enhanced electron precipitation [e.g., *Rosenberg et al.*, 1971; *Inan et al.*, 1985; *Gamble et al.*, 2008; *Parrot et al.*, 2007; *Savaud et al.*, 2008], but to date, there have been no direct optical observations to confirm the nature of the electron precipitation during individual events.

2. Observations and Results

An observational campaign to detect optical signatures induced by the 16.4 kHz JXN transmitter (~67°N, ~14°E) was carried out in January 2012. A static camera system was deployed close to Bodø, Norway, ~40 km from the JXN transmitter which transmits with a reported power of ~150 kW [*Barr*, 1996]. The system comprises an Andor DU-888 camera with Electron Multiplying Charge Coupled Device (EMCCD) providing a field-of-view of ~30° of sky, centered on the zenith, with recordings taken at 10 frames per second with a digital resolution of 256 × 256
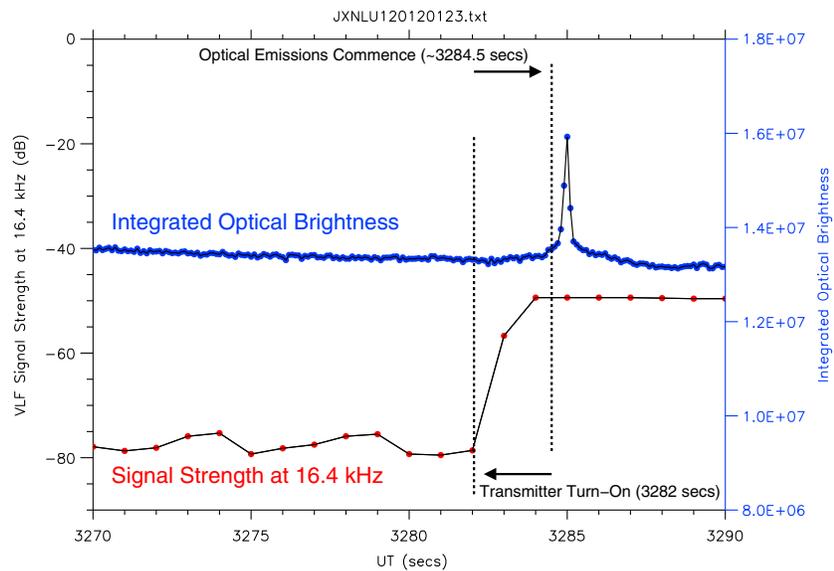
Figure 2. Enlarged view of 20 s of observations around the time of turn-on of the JXN transmitter. The figure shows the approximate timing for turn-on of the JXN transmitter and the commencement of enhanced optical observations.

pixels. This field-of-view (FOV) corresponds to a spatial radius of ~26 km of sky at 100 km altitude. The timing accuracy of <0.1 s was determined by coupling to a GPS antenna. The camera was fitted with a 25 mm lens ($F = 0.85$) and was filtered with one of two separate filters; a >6450 Å long pass filter (that captures emissions between 6450 and ~8500 Å or a 4278 Å narrowband filter (100 Å width). 4278 Å is a prompt band emission that is produced by electrons with energies higher than 14.5 eV impacting N_2 molecules with the radiative lifetime of the band ~6×10^{-8} s [*Bennett and Dalby*, 1959].

Monitoring of the VLF transmissions from JXN (magnetic inclination ~76°), and a number of other VLF transmitters, is routinely made by VLF radio receivers forming part of the Antarctic-Arctic Radiation-belt (Dynamic) Deposition - VLF Atmospheric Research Konsortium (AARDDVARK) network [*Clilverd et al.*, 2009]. In this instance monitoring of the JXN transmissions was made from an AARDDVARK receiver located on the east coast of the UK [*Kavanagh et al.*, 2011] at a cadence of 1 s (with ±1 s accuracy). During the observational campaign, the JXN transmitter was cycling through a 1 h on and 3 h off transmission pattern which was common for this transmitter during 2012, although no further knowledge of the transmitter/antenna set-up were obtained. To detect any increase in electron precipitation caused by the VLF transmissions, the optical brightness of the sky was imaged before, during, and after a selection of turn-ons of the JXN transmitter using two optical filters. Observations were carried out for eight turn-ons of the JXN transmitter, six of these using the >6450 Å filter, and two using the 4278 Å filter. No change in optical emissions was noted using the >6450 Å filter. For the two occasions using the 4278 Å filter (both on 23 January 2012), only the first occasion resulted in detection of an increase in optical emissions. The presence of natural aurora and airglow resulted in an elevated background brightness during the second occasion.

Figure 1 contains a summary of the observations during the first turn-on of the JXN transmitter on 23 January 2012. The *x* axis in Figure 1 indicates the number of seconds from 0:00 UT, while the *y* axis indicates the measured VLF signal strength at 16.4 kHz (in dB) and the integrated optical brightness (in arbitrary units) at 4278 Å during the observational period. The optical brightness is the sum of the charge-coupled device measured intensity of each individual pixel in the image—absolute calibration of the optical system has not been carried out. Observations were carried out prior-to and during a period with elevated geomagnetic activity when natural aurorae were present. The aurorae caused fluctuations in the measured optical brightness and in the measured VLF signal strength, particularly after ~4000 s (Figure 1, top). (Note: see *Clilverd et al.* [2009] for further discussion of how this diagnostic can be used to infer energetic particle precipitation along the raypath between VLF transmitter and receiver). However, the main feature of interest for this study can be found upon examination of the period around transmitter turn-on at ~3282 s. The
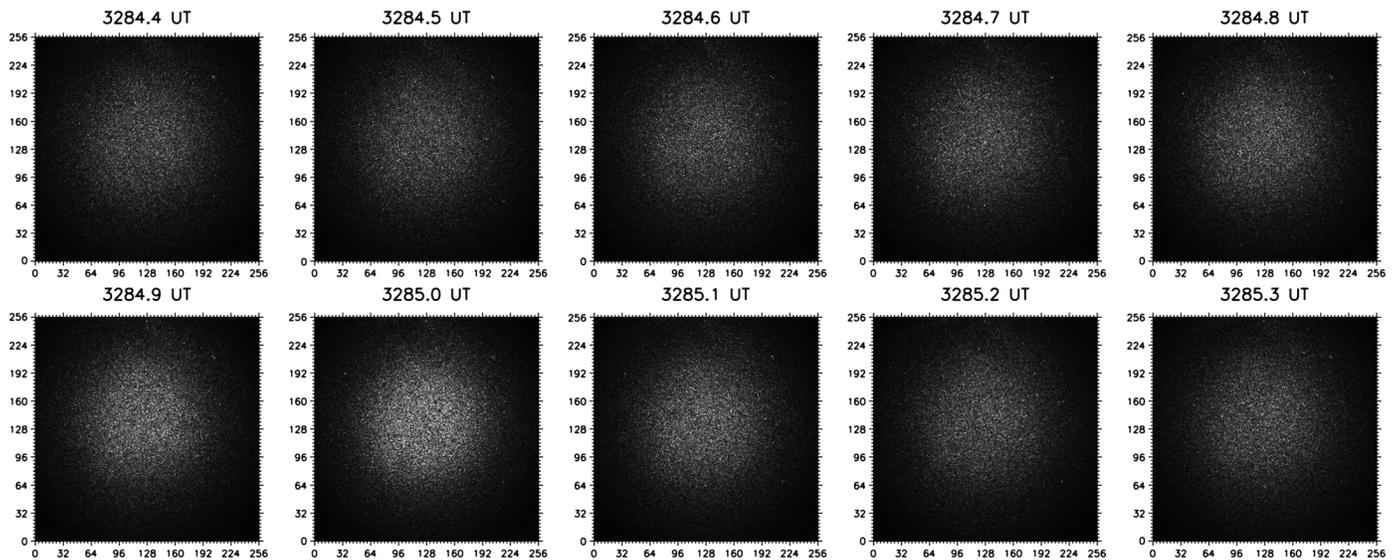
Figure 3. Ten frames (1 s) of optical observations (256 × 256 pixels) at 4278 Å following turn-on of the JXN transmitter. The field-of-view is approximately ±15° which corresponds to ~26 km in the sky at 100 km altitude. The peak in optical brightness occurs at 3285.0 UT, is centered on the zenith, and has no discernable structure.

observations indicate a sudden and temporary increase in the measured optical brightness just after turn-on of the JXN transmitter (Figure 1, bottom). The temporal changes in optical brightness around turn-on are of a substantially different character from those due to natural auroral emissions seen later in the evening. In addition, it is clear that the transient optical signal observed close to turn-on is substantially less than the brightness of the emissions resulting from natural aurora later the same evening.

Figure 2 contains a plot of the 20 s of data around the time of transmitter turn-on and provides a detailed view of the >20% change in the measured optical brightness during this period. The transmitter turn-on occurred at ~3282.0 s with a sharp increase in measured optical brightness commencing approximately 2.5 ± 1.0 s later at ~3284.5 ± 1.0 s with the elevated optical emissions lasting around 0.5 s.

Figure 3 contains plots showing 10 frames of the optical brightness across the camera field-of-view around the turn-on of the transmitter. The figure provides an indication of the spatial extent of the emissions and demonstrates that (a) emissions are enhanced over the entire camera field-of-view, (b) emissions appear to be centered on the zenith, and (c) emissions do not exhibit any detectable spatial structure.

3. Discussion and Conclusions

Given the extensive modeling work already carried out in this area [e.g., *Inan et al.*, 2003; *Kulkani et al.*, 2008] and various particle detection observations [e.g., *Rosenberg et al.*, 1971], it is difficult to conclude that the optical signature observed during this campaign is caused by anything other than the VLF waves at 16.4 kHz transmitted by JXN interacting with the in situ electron population in the magnetosphere. Only one observation of this phenomenon has been carried made, although other possible causes for the transient optical signal have been considered (e.g., the transmitter somehow connecting electromagnetically with the camera/data logger) and ruled out (e.g., by carrying out observations of a turn-on with the lens cap on). It is noted that changes in measured brightness due to the headlamps of cars passing the observing site are easy to spot in the data and have been discarded as a possible cause. In addition, no lightning storms were reported in the region around the time of the observations.

Above the ionosphere, the 16.4 kHz wave produced following turn-on of the transmitter might be expected to be guided along the magnetic field [*Inan et al.*, 2003]. However, at this location, calculations show the wave will not be ducted. As pointed out by *Rodger et al.* [2010], there remains uncertainty in the community as to whether ducted or nonducted waves are most significant for loss processes [see also *Clilverd et al.*, 2008; *Kulkani et al.*, 2008]. Assuming off-equatorial gyro-resonance, then at some point along the field line, the wave frequency will match the cyclotron frequency of a proportion of the electron distribution and scattering

will occur, resulting in some electrons entering the atmospheric loss cone. Once within the atmosphere, the precipitating electrons will collide with atmospheric neutral particles to produce airglow: 4278 Å airglow is produced by electrons with energies >14.5 eV impacting N_2 molecules [*Bennett and Dalby*, 1959]. *Rosenberg et al.* [1971] previously obtained evidence for electron precipitation close to the Siple station on Antarctica ($L = 4.1$) from electrons with energies >~30 keV. The electrons in that case, during enhanced geomagnetic activity, were detected by sodium iodide scintillation counters several tenths of a second following the emission of a burst of VLF waves with frequencies of a few kHz.

The location of the cyclotron-resonance region in the magnetosphere and the propagation time between the ionosphere and that resonance region for a 16.4 kHz electromagnetic signal were estimated by (a) modeling the magnetic field and the total electron density of the ionosphere and magnetosphere and (b) using cold-plasma theory to estimate the propagation velocity of electromagnetic plasma waves (whistlers). A propagation time of 0.49 s was obtained for the 16.4 kHz JXN transmitter and its 16.4 kHz resonance region a distance of 21,000 km away along the magnetic field line. This propagation time is mostly due to a reduced group velocity in the ionosphere and to a reduced group velocity as the wave approaches the cyclotron resonance region. For hot magnetospheric electrons that are pitch-angle scattered into the atmospheric loss cone in the region of cyclotron interaction, the flight time along a spiraling orbit from the interaction region down to the atmosphere is estimated to be 0.6–1.3 s. Adding these two times together (the time for the electromagnetic signal to propagate upward and the time for an electron to transit downward), the estimated time for the airglow to turn on after the transmitter is 0.49 s plus 0.6 to 1.3 s. This yields a time-to-airglow of between 1.1 s and 1.8 s. This time scale is consistent with that observed in the experimental observations.

One feature of the observations is that the enhanced optical emissions are short-lived and that following an initial burst of precipitation, the measured optical brightness returns close to its preturn-on level. At least two possibilities exist: (1) Following an initial burst of precipitation, the source and loss of the electrons in the outer radiation belt will reach a new equilibrium (as suggested by *Inan et al.* [2003]) with the loss of electrons creating an anisotropic distribution which could drive instabilities. Such instabilities may then accelerate lower energy electrons back up to energies which were previously removed—a process which would allow the overall balance between source and loss to tend to a constant level, after an initial burst of precipitation. (2) When the transmitter is off, there will exist a population of electrons with pitch angles just above the bounce-loss cone. When the transmitter then turns on, this population is rapidly scattered generating the initial burst of precipitation. Electrons with initial pitch angles further from the bounce-loss cone would subsequently scatter more slowly and take longer to precipitate. Calculations of the time required for both (1) and (2) indicate these processes should take at least several seconds whilst the optical signature lasts less than 1 s.

In the current study, only the 4278 Å filter produced a positive signal. However, we speculate that detectable emissions may exist at other wavelengths (e.g., 5577 Å or 7774 Å) around turn-on but these will require narrowband filters to detect, rather than the long pass >6450 Å filter used during the observational campaign described above. Given that the optical system used has not been calibrated for absolute brightness, we have no straight-forward way to estimate the photon flux incident on the camera, or the precipitating electron flux ultimately responsible. However, the arguments and calculations outlined by *Marshall et al.* [2010] indicate that the signal-to-noise ratio at 4278 Å should only be detectable statistically over many events. The observation described above suggests otherwise, although replication of the observed transient optical signal in other campaigns is necessary to confirm this. Interpretation of the experimental result described in this paper remains challenging.

4. Summary

To summarize, a campaign to detect observational signatures of electron precipitation due to transmissions at 16.4 kHz from a powerful VLF transmitter revealed a short-lived increase in the measured optical brightness at 4278 Å occurring around 2.5 ± 1.0 s after the transmitter was turned on. Such observations are consistent with precipitation of electrons from the outer magnetosphere. The observed precipitation is centered on the zenith and has no detectable spatial structure. We conclude that the VLF waves generated by the JXN transmitter are traveling out into the magnetosphere, where they resonantly interact with, and

cause pitch angle scattering of, the in situ magnetospheric electron population. This sequence of events is somewhat supported by previous modeling work and the calculations described above. The result outlined here demonstrates that precipitation of electrons from flux tubes can be stimulated using powerful VLF transmitters. It is noted that the experiment described above makes no attempt to tune the transmitted VLF wave. Given the full capabilities of a powerful VLF transmitter, it should be possible to vary the transmitted wave to resonate with different energies at different points along the magnetic field line. Tuning of the transmitted wave would likely significantly enhance the number of electrons that were subject to pitch-angle scattering, and could thus increase the number of electrons from each flux tube which would precipitate into the atmosphere. Further such experiments are planned at JXN and at other VLF transmitters (with different transmission frequencies).

References

Abel, B., and R. M. Thorne (1998), Electron scattering loss in Earth's inner magnetosphere 1. Dominant physical processes, *J. Geophys. Res.*, *103*, 2385–2396.

Baker, D. N., J. B. Blake, L. B. Callis, J. R. Cummings, D. Hovestadt, S. Kanekal, B. Klecker, R. A. Mewaldt, and R. D. Zwickl (1994), Relativistic electron acceleration and decay time scales in the inner and outer radiation belts: SAMPEX, *Geophys. Res. Lett.*, *21*, 409–412.

Barr, R. (1996), VLF wave generation using VLF heating and the cubic nonlinearity of the ionosphere, *Geophys. Res. Lett.*, *23*, 2165–2168.

Bell, T. F., J. P. Katsufrakis, and H. G. James (1985), A new type of VLF emission triggered at low altitude in the subauroral region by Siple station VLF transmitter signals, *J. Geophys. Res.*, *90*, 12,183–12,194.

Bennett, R. G., and F. W. Dalby (1959), Experimental determination of the oscillator strength of the first negative bands of N_{2+}, *J. Chem. Phys.*, *31*, 434.

Clilverd, M. A., C. A. Rodger, R. J. Gamble, N. P. Meredith, M. Parrot, J.-J. Berthelier, and N. R. Thomson (2008), Ground-based transmitter signals observed from space: Ducted or nonducted, *J. Geophys. Res.*, *113*, A04211, doi:10.1029/2007JA012602.

Clilverd, M. A., et al. (2009), Remote sensing space weather events: The AARDDVARK network, *Space Weather*, *7*, S04001, doi:10.1029/2008SW000412.

Dungey, J. W. (1963), Loss of Van Allen electrons due to whistlers, *Planet. Space Sci.*, *11*, 591–595.

Gamble, R. J., C. J. Rodger, M. A. Clilverd, J.-A. Sauvaud, N. R. Thomson, S. L. Stewart, R. J. McCormick, M. Parrot, and J.-J. Berthelier (2008), Radiation belt precipitation by man-made VLF transmissions, *J. Geophys. Res.*, *113*, A10211, doi:10.1029/2008JA013369.

Helliwell, R. A., J. P. Katsufrakis, and M. L. Trimpi (1973), Whistler-induced amplitude perturbation in VLF propagation, *J. Geophys. Res.*, *78*, 4679–4688.

Hess, W. N. (1968), *The Radiation Belt and Magnetosphere*, Blaisdell, London.

Inan, U. S., H. C. Chang, and R. A. Helliwell (1984), Electron precipitation around major ground-based VLF signal sources, *J. Geophys. Res.*, *89*, 2891–2906.

Inan, U. S., D. L. Carpenter, R. A. Helliwell, and J. P. Katsufrakis (1985), Subionospheric VLF/LF phase perturbations produced by lightning-whistler induced particle precipitation, *J. Geophys. Res.*, *90*, 7457–7469.

Inan, U. S., T. F. Bell, J. Bortnik, and J. M. Albert (2003), Controlled precipitation of radiation belt electrons, *J. Geophys. Res.*, *108*(A5), 1186, doi:10.1029/2002JA009580.

Kavanagh, A. J., M. H. Denton, J. Denton, and H. Harron (2011), Probing geospace with VLF radio signals, *Astron. Geophys.*, *52*, 2.27–2.30.

Koons, H. C., B. C. Edgar, and A. L. Vampola (1981), Precipitation of inner zone electrons by whistler mode waves from VLF transmitters UMS and NWC, *J. Geophys. Res.*, *86*, 640–648.

Kulkani, P., U. S. Inan, and T. F. Bell (2008), Energetic electron precipitation induced by space based VLF transmitters, *J. Geophys. Res.*, *113*, A09203, doi:10.1029/2008JA013120.

Marshall, R. A., R. T. Newsome, N. G. Lehtinen, N. Lavassar, and U. S. Inan (2010), Optical signatures of radiation belt electron precipitation induced by ground-based VLF transmitters, *J. Geophys. Res.*, *115*, A08206, doi:10.1029/2010JA015395.

Parrot, M., J. A. Savaud, J. J. Berthelier, and J. P. Lebreton (2007), First in-situ observations of strong ionospheric perturbations generated by a powerful VLF ground-based transmitter, *Geophys. Res. Lett.*, *34*, L11111, doi:10.1029/2007GL029368.

Rodger, C. J., M. A. Clilverd, T. Ulich, P. T. Verronen, E. Turunen, and N. R. Thomson (2006), The atmospheric implications of radiation belt remediation, *Ann. Geophys.*, *24*, 2025–2041.

Rodger, C. J., B. R. Carson, S. A. Cummer, R. J. Gamble, M. A. Clilverd, J. C. Green, J.-A. Sauvaud, M. Parrot, and J.-J. Berthelier (2010), Contrasting the efficiency of radiation belt losses caused by ducted and nonducted whistler-mode waves from ground-based transmitters, *J. Geophys. Res.*, *115*, A12208, doi:10.1029/2010JA015880.

Rosenberg, T. J., R. A. Helliwell, and J. P. Katsufrakis (1971), Electron precipitation associated with discrete very-low frequency emissions, *J. Geophys. Res.*, *76*, 8445–8452.

Savaud, J.-A., R. Maggiolo, C. Jacquey, M. Parrot, J.-J. Berthelier, R. J. Gamble, and C. J. Rodger (2008), Radiation belt electron precipitation due to VLF transmitters: Satellite observations, *Geophys. Res. Lett.*, *35*, L09101, doi:10.1029/2008GL033194.

Van Allen, J. A., G. H. Ludwig, E. C. Ray, and C. E. McIlwain (1958), Observation of high intensity radiation by satellites 1958 Alpha and Gamma, *Jet Propul.*, *28*, 588–592.

Wrenn, G. L. (2009), Chronology of "killer" electron: Solar cycles 22 and 23, *J. Atmos. Sol. Terr. Phys.*, *71*, 1210–1218, doi:10.1016/j.jastp.2008.08.002.